



HAL
open science

Automated classification of Plasmodium sporozoite movement patterns reveals a shift towards productive motility during salivary gland infection

Stephan Josef Hegge, Mikhail Kudryashev, Ashley Smith, Friedrich Frischknecht

► **To cite this version:**

Stephan Josef Hegge, Mikhail Kudryashev, Ashley Smith, Friedrich Frischknecht. Automated classification of Plasmodium sporozoite movement patterns reveals a shift towards productive motility during salivary gland infection. *Biotechnology Journal*, 2009, 4 (7), pp.903. 10.1002/biot.200900007. hal-00484738

HAL Id: hal-00484738

<https://hal.science/hal-00484738>

Submitted on 19 May 2010

HAL is a multi-disciplinary open access archive for the deposit and dissemination of scientific research documents, whether they are published or not. The documents may come from teaching and research institutions in France or abroad, or from public or private research centers.

L'archive ouverte pluridisciplinaire **HAL**, est destinée au dépôt et à la diffusion de documents scientifiques de niveau recherche, publiés ou non, émanant des établissements d'enseignement et de recherche français ou étrangers, des laboratoires publics ou privés.



Automated classification of *Plasmodium* sporozoite movement patterns reveals a shift towards productive motility during salivary gland infection

Journal:	<i>Biotechnology Journal</i>
Manuscript ID:	biot.200900007.R1
Wiley - Manuscript type:	Research Article
Date Submitted by the Author:	05-Mar-2009
Complete List of Authors:	Hegge, Stephan; Heidelberg University School of Medicine, Department of Parasitology Kudryashev, Mikhail; Heidelberg University School of Medicine, Department of Parasitology Smith, Ashley; Rice University Frischknecht, Friedrich; Heidelberg University School of Medicine, Department of Parasitology
Keywords:	object tracking, gliding motility, Plasmodium sporozoite, malaria



Research Article ((6808 words))**Automated classification of *Plasmodium* sporozoite movement patterns reveals a shift towards productive motility during salivary gland infection**

Stephan Hegge*, Mikhail Kudryashev*, Ashley Smith and Friedrich Frischknecht

*contributed equally

Department of Parasitology, Hygiene Institute, University of Heidelberg Medical School,
Im Neuenheimer Feld 324, 69120 Heidelberg, Germany

Correspondence: Friedrich Frischknecht, Department of Parasitology, Hygiene Institute,
University of Heidelberg Medical School, Im Neuenheimer Feld 324, 69120 Heidelberg,
Germany

tel: 49-6221-566537

fax: 49-6221-564643

email: freddy.frischknecht@med.uni-heidelberg.de

keywords: object tracking, gliding motility, *Plasmodium* sporozoite, malaria

Abstract

The invasive stages of malaria and other apicomplexan parasites use a unique motility machinery based on actin, myosin and a number of parasite specific proteins to invade host cells and tissues. The crucial importance of this motility machinery at several stages of the live cycle of these parasites makes the individual components potential drug targets. The different stages of the malaria parasite exhibit strikingly diverse movement patterns, likely reflecting the varied needs to achieve successful invasion. Here we describe a Tool for Automated Sporozoite Tracking (ToAST) that allows the rapid simultaneous analysis of several hundred motile *Plasmodium* sporozoites, the stage of the malaria parasite transmitted by the mosquito. ToAST reliably categorizes different modes of sporozoite movement and can be used for both tracking changes in movement patterns and comparing overall movement parameters, such as average speed or the persistence of sporozoites undergoing a certain type of movement. This allows the comparison of potentially small differences between distinct parasite populations and will enable screening of drug libraries to find inhibitors of sporozoite motility. Using ToAST we find that isolated sporozoites change their movement patterns towards productive motility during the first week after infection of mosquito salivary glands.

1 Introduction

Pathogens often rely on their own motility (e.g. bacterial flagellar motion) to enter host organisms and cells [1-6]. In the case of malaria, the *Plasmodium* parasite relies on a motility apparatus at different stages of the life cycle that is based on an actin-myosin motor and the retrograde capping of secreted surface adhesins [7-9]. *Plasmodium* merozoites bind to red blood cells and enter them actively by means of this motor before replicating within the cell [10]. Within the mosquito gut, motile ookinetes can penetrate the epithelium. Like merozoites, ookinetes rely on the actin-myosin motor to move, but they do not invade an epithelial cell to remain intracellular. Instead ookinetes migrate through epithelial cells and form a cyst at the basal side of the epithelium [11]. Within this cyst, *Plasmodium* sporozoites develop and eventually enter the salivary glands to be transmitted back to the host during a mosquito bite [12]. Similar to other arthropod-borne disease agents, the majority of sporozoites are injected into the skin, while a few might directly enter the blood stream [13-20]. While sporozoites within the salivary gland rarely move, those transmitted into the skin move at high speed [14, 21, 22]. Some of those transmitted sporozoites actively enter blood vessels and penetrate the liver parenchym, where they eventually invade hepatocytes to multiply into thousands of merozoites [23]. Clearly, to inhibit sporozoite motility means to interrupt transmission of the disease, as the parasite is not able to reach and invade hepatocytes [12, 24].

Plasmodium sporozoites also move *in vitro* [25, 26]. Sporozoites isolated from infected salivary glands can undergo attached waving, a movement not associated with translocation, where the parasite is attached with one end and waves with its body in the medium [26]. Little is known about the molecular base of this movement. Alternatively, these sporozoites can undergo actin and myosin-dependent gliding motility, whereby they translocate without changing their shape [7, 25, 26]. Sporozoites are highly polarized and crescent shaped cells, which glide with their apical (front) end leading. *In vitro* sporozoites move in circles with one preferred direction [26]. This makes them amenable for visual analysis like almost no other cell, as it allows long-term observation of single parasites moving for up to dozens of minutes without leaving the field of view. Here, we developed a tracking tool that allows the classification of movement patterns and other parameters describing sporozoite motion. This tool will also enable us to conduct a high

throughput search for inhibitors targeting the gliding motility machinery.

2 Materials and Methods

2.1 Parasites and microscopy

Plasmodium berghei (strain NK65) sporozoites expressing green fluorescent protein [27] were produced in *Anopheles stephensi* mosquitoes essentially as described previously [21]. Salivary glands were dissected and sporozoites isolated in a 1,5 ml reaction tube containing RPMI tissue culture medium with 3% bovine serum albumin. For imaging sporozoites were placed in a well of a 384 well plate (Corning, flat bottom, black with 0.9 mm clear polystyrene bottom, Wiesbaden, Germany). Plates were centrifuged (room temperature, 200 g, 3 min) and imaging was performed on an inverted Axiovert 200M Zeiss microscope in an air-conditioned imaging suite at room temperature (24°C) or at 37°C in a heated incubator (part of the Zeiss CellObserver system). Images were collected with a Zeiss AxioCam HRm every 1 or 2 seconds using Axiovision 4.6 software and various objective lenses (10 x Apoplan objective (NA 0,25) or 63x Plan-Apochromat (NA 1.40)). All image series were eventually imported to ImageJ for analysis and figures were generated using the Adobe Creative Suite software package.

2.2 Image processing:

2.2.1 Local thresholding for signal detection.

For each frame in a time-lapse image series, the mean (M) pixel value and average deviation from the mean (AD) were calculated and the global threshold of $M+nAD$ was applied for each picture separately (this was implemented as "the Thresholder plugin") with typical values for $n = 5, 7, 9$. Pictures were processed separately as the overall intensity may have decreased over the time of acquisition due to photobleaching. Adjacent pixels were segmented into one object.

2.2.2 Automatic sporozoite tracking.

Particle tracking was essentially performed with the MTrack2 plugin implemented by Nico Stuurman [<http://valelab.ucsf.edu/~nico/IJplugins/MTrack2.html>]. It identifies the objects in each frame of a thresholded movie and determines which objects in the

1
2
3 successive frames are closest together. If these are located within a user defined distance
4 limit then these objects are assembled to a track. In order to distinguish sporozoites from
5 mosquito salivary gland tissue debris that occasionally may be present in the movies, we
6 introduced a spherical factor (SPF) of an object as a correlation coefficient between x and
7 y coordinates of all object pixels in a coordinate system tilted 45 degrees to the principal
8 axis of the object. The SPF varies from 0 for a round object to 1 for an ideal line and is
9 typically 0.75 to 0.9 for a sporozoite. For our analysis, all objects with an average SPF
10 below 0.4 for the whole track length were removed from the resulting log-file.
11
12
13
14
15
16
17

18 19 **2.2.3 Classification of sporozoite motility patterns.**

20
21 The translational speed V and the rotational speed α for each time point for each parasite
22 was calculated from the coordinates, pixel size and time interval between frames. Next,
23 averaging over $2k+1$ (k is the sliding average half-size, a user defined parameter with a
24 typical value of 4 for 0.5 hz image series) consecutive time points for every track was
25 performed. The averaging reduced the noise present in a low magnification image series
26 and thus yielded more reliable values for v and α . All objects with an average velocity
27 below $v_{\min} \leq 0.5$ micrometers per second were assigned as “attached” parasites. All
28 objects having an average *absolute* value of $\alpha \leq V/45$ were assigned as gliders, all the
29 others were assigned as wavers with 45 corresponding to the angle of the separation line
30 between gliders and wavers. This number was empirically determined to minimize the
31 error in automated versus manual annotation. Then gliders were sub-classified into either
32 counter-clockwise (CCW), which is gliding with a negative average angle increment, or
33 clockwise (CW), gliding (positive average angle increment). The steps described under
34 2.2.2 and 2.2.3 were implemented into our ImageJ plugin “ToAST”, which is available
35 on request.
36
37
38
39
40
41
42
43
44
45
46
47
48
49

50 **2.2.4 Processing of multiple movie files.**

51
52 Processing of multiple image series was performed by an ImageJ macro in the following
53 steps: movie files with consistent filenames were loaded, (semi)automatically thresholded
54 by the “thresolder plugin” (user has to set the number of average deviations based on the
55 quality of the signal) and processed via “ToAST”. The resulting tracking output of every
56
57
58
59
60

1
2
3 movie was stored in a text-file, together with the thresholded and tracked movies and a
4 tiff-image showing the paths of all assigned tracks. The original files remain unmodified.
5
6 The data visualisation was accomplished with a Microsoft Excel macro.
7
8
9

10 **2.3 Error estimation**

11 “Easy-to-classify parasites” that followed the same motility pattern over the whole
12 duration of observation were first manually assigned to the motility states in the
13 following way: the percentage of gliding, waving and being attached was assigned for
14 every parasite. The overall percentage for 6 parasites showing simple motility patterns
15 was compared to the results of automatic assignment.
16
17

18 “Difficult-to-classify parasites” that frequently changed their motility patterns were
19 assigned to the motility states frame by frame by several non-experienced and
20 experienced users asked to memorize only the 3 previous time frames. Then, for every
21 time point a consensus-assignment was made if most of the users agreed on one of the
22 states, otherwise the respective time points remained unannotated. Finally, manual
23 assignment was compared to the automatic annotation.
24
25
26
27
28
29
30
31
32

33 **3 Results**

34 **3.1 Distinct sporozoite movement patterns**

35 To visualize moving *Plasmodium* sporozoites, we isolated parasites expressing
36 cytoplasmic GFP from mosquito salivary glands. Imaging was performed with a variety
37 of frame rates on a wide-field fluorescence microscope with either 10x or 63x objective
38 lenses (pixel size: 627x627 and 98x98 nm², respectively). High magnification imaging
39 readily revealed the different movement patterns: (i) drifting, which describes parasites
40 not yet adherent on the substrate; (ii) attached, which describes sporozoites adherent with
41 one end and the other end showing only small displacements; (iii) waving, which
42 describes parasites attached with one end to the substrate and the other end moving
43 actively in the medium; (iv) gliding in a counter-clockwise (CCW) direction and (v)
44 gliding in a clockwise (CW) direction (Fig 1). These distinct parasite movement patterns
45 could also be reliably observed with a 10x objective allowing simultaneous tracking up to
46 250 sporozoites (Fig 2A-C). Thresholding of the fluorescent signal and maximum
47
48
49
50
51
52
53
54
55
56
57
58
59
60

1
2
3
4
5
6
7
8
9
10
11
12
13
14
15
16
17
18
19
20
21
22
23
24
25
26
27
28
29
30
31
32
33
34
35
36
37
38
39
40
41
42
43
44
45
46
47
48
49
50
51
52
53
54
55
56
57
58
59
60

fluorescent intensity projections allowed the visualization of movement patterns and formed the basis for quantitative analysis. Projections of movies over only 20 frames recorded at 1 Hz showed mainly homogenous patterns of movements (Fig 2D, white projections), while projections over longer periods of time (Fig 2D, red projections) revealed that parasites did not just undergo one type of movement, but could switch between different movements (Fig 2D, white and red projections) as originally reported [26].

3.2 Tracking motile parasites

As drifting does not describe an active movement of the parasites and we anticipated problems of differentiating between this and other types of movement, we centrifuged the parasites at 200g for 3 minutes, which abrogated floating while the other movement patterns were still observed. To determine the speed of sporozoites we compared the results of different manual approaches using the Manual Tracking tool of ImageJ (Mtrack) to those derived by the automatic Mtrack2 plug-in. We tracked the same sporozoites acquired at 100x with 0.5 Hz in four different ways. 1. Manual tracking of the front end of the sporozoite one time each by 3 different users (Fig 3B, 1t 3p); 2. Manual tracking of the front end of the sporozoite by the same user repeated three times (Fig 3B, 3t 1p); 3. Manual tracking of the center of the sporozoite by one user repeated three times (Fig 3B, 3t 1p); 4. Automated tracking of the sporozoite's center (Mtrack2) with different threshold values, namely 3, 5 and 7 average deviations using the 'automatic thresholder' plug-in (Fig 3B, 3thr Mac). All four approaches showed differences in speed from one measurement of the same frame to another. However, the lowest standard deviation was observed for automated tracking, which also resulted in the lowest average speed (Fig 3B). This apparent decrease in speed is due to waving behaviors between gliding intervals as a waving sporozoite shows smaller displacements at the center than at the tip. In perfectly circular gliding sporozoites, no difference in average speed is detected (data not shown). Intuitively, imaging at low frequency decreases the speed of the circular moving parasites (Fig 3C). However, an increase in sampling rate will not indefinitely improve the measurement, as at high frame rates the tracking error will eventually cause an artificial increase in the tracked distance covered by a moving object (Fig 3D and S.

Münter, M. Kudryashev, S. Hegge and F. Frischknecht, unpublished data).

3.3 Automated classification of movement patterns

In order to test the possibility of distinguishing between the different patterns of movement, including those that do not contribute to active locomotion, we investigated 100 consecutive frames imaged at 1 Hz and manually assigned sporozoites showing either simple or more complex linear combinations of the described patterns (Fig 3E). The variability of manual tracking was assessed by different users. Persons who never classified parasites before, termed inexperienced users, as well as experienced users who have regularly tracked and classified sporozoites previously, were asked to assign one of the four different movement features to the same set of parasites. Subsequently, the agreement between these two groups of users was measured by the number of identically assigned frames (Fig 3F). This yielded a larger observer error than simple tracking of gliding sporozoites. As expected, classifying “easy-to-classify” parasites yielded the highest agreement between all sets of users and served as a control. More difficult patterns of movement, namely when a sporozoite switched the type of movement several times, resulted in a lower overall agreement, although experienced users had a higher agreement than inexperienced users. Surprisingly, waving parasites never showed matches better than 60%. Analysis of the raw data revealed that human judgment varies the most when trying to distinguish between passive motion of a sporozoite, which then would be mistakenly assigned as ‘attached’, and slow active motion, which then would be assigned as ‘waving’. This error between observers was particularly apparent when parasites underwent frequent changes between movement patterns (e.g. gliding CW followed by waving followed by gliding CCW etc).

In order to computationally distinguish between these patterns, we calculated the translational speed v as the distance between the center of the same parasite in two consecutive frames and the relative angle increment α between the directions of two consecutive displacement moves of a parasite (Fig 4A) and plotted one against the other (Fig 4B). Parasites undergoing gliding motility were characterized by high speed that on average related linearly to the absolute value of rotational speed for every single sporozoite. Next, sporozoites gliding clockwise could be distinguished from those gliding

1
2
3
4 counter-clockwise when the exact value and the sign of the rotational speed was plotted
5 against the translational speed (Fig 4C-E). Parasites that were attached showed little
6 displacement at very low speed, while those undergoing waving motion underwent a
7 range of angular displacements at an intermediary speed (Fig 4B). In order to reduce the
8 noise from automated tracking we employed averaging of translational and rotational
9 speeds over $2n+1$ time frames (Fig 4B). For our imaging conditions we set n to be 4 to 8.
10 Finally, in order to quantify the number of different states of movement in a population
11 over the time of observation we counted the number of points in each area (Fig 4B).
12 Examination of parasites that showed a range of different movements revealed that this
13 way of distinguishing between patterns provided only a rough estimate, and relied on a
14 manual setting of the borders that delineated the data-points into a particular category.
15 However, as the attached parasites resulted in a cloud of points that always fell in the
16 range below $0.5\mu\text{m/s}$, we delineated attached sporozoites from the others at this speed
17 (Fig 4B). Sporozoites moving in circles showed a correlation between the translational
18 and rotational speed of about 0.95 that made the dependence in the scatter for every
19 single track close to linear. Maximal observed angles of inclination of the v/α line never
20 exceeded $0.02\mu\text{m}/(\text{s} \times \text{degree})$, which made it possible to computationally isolate gliding
21 parasites. Waving sporozoites showed high variation in both translational and rotational
22 speeds and thus were the hardest to classify both manually and computationally. The
23 whole procedure from loading the stored movies till visualization of the result windows
24 in Excel was called a Tool for Automated Sporozoite Tracking (ToAST) (Fig 4F).
25
26
27
28
29
30
31
32
33
34
35
36
37
38
39
40
41
42

3.4 Automated versus manual assignment of movement types

43
44 Comparison of automated classification with user-based assignments for “difficult-to-
45 classify” parasites revealed a better agreement for the identification of attached and
46 motile states than for wavers by both inexperienced and experienced users (Fig 5A). As
47 expected, experienced users had a higher match to the automated procedure results. Still,
48 the overall reliability of classification of parasites exhibiting complex movement patterns
49 was low.
50
51
52
53
54

55 However, these difficult-to-classify sporozoites constitute only a small minority of the
56 imaged population ($\leq 5\%$, see Fig 2D). Therefore, comparing the automated classification
57
58
59
60

1
2
3 (automatic thresholding applying 5, 7 and 9 average deviations) to the annotation by 3
4 experienced users for an entire movie (100 frames at 1 Hz) containing over 100
5 sporozoites showed that the overall classification is highly reliable (Fig 5B). Less
6 reliability might be observed when ToAST is applied on other parasites such as *T. gondii*
7 tachyzoites, which change movement patterns more frequently.
8
9
10
11
12
13

14 **3.5 ToAST reveals a shift of movement patterns during sporozoite maturation**

15 We applied ToAST to test a number of different sporozoite preparations derived from
16 infected mosquitoes at different days after the mosquitoes received their infective blood
17 meal. First we tested whether sporozoites from mosquitoes dissected at the same time
18 show different movement patterns and average speeds if separated in classes of “low
19 level” and “high level” salivary gland infection. We found no difference in any of the
20 tested movement parameters, including overall sporozoite speed (Fig 6A,B). When
21 sporozoites were imaged at room temperature or at 37°C the percentage of productive
22 gliders dropped faster at higher temperature (Fig 6C). Gliding sporozoites moved
23 consistently faster at higher temperature, but the speed of those moving at room
24 temperature remained constant over a longer time (Fig 6D). As sporozoites are thought to
25 mature within the salivary glands and rarely move when isolated from midguts [12], we
26 next tested sporozoites isolated from mosquitoes at the same day from midguts,
27 hemolymph and salivary glands. This confirmed the previous observations and showed
28 that some sporozoites isolated from hemolymph moved by active gliding, while those in
29 the salivary glands moved faster (Fig 6 E,F). When sporozoites were taken at early days
30 (day 13) after infection and compared with sporozoites taken from the same infected
31 batch of mosquitoes 6 days later it was found that 20% of day 13 sporozoites were
32 gliding while at day 19 the proportion of movers increased to 50%. Concomitantly, the
33 proportion of attached sporozoites decreased (Fig 6G). This shows that ToAST is able to
34 reveal differences between sporozoite populations and could in principle be useful for
35 analyzing effects of different concentrations of drugs that inhibit motility. Indeed,
36 investigating the actin dynamics inhibiting drug cytochalasin D, which has been long
37 known to inhibit apicomplexan parasite motility, rapidly confirmed that increasing drug
38 concentrations decreased the number of sporozoites undergoing active gliding motility
39
40
41
42
43
44
45
46
47
48
49
50
51
52
53
54
55
56
57
58
59
60

(Fig 6H) [28].

4 Discussion

4.1 Towards automated tracking of *Plasmodium* sporozoites

We established a **T**ool for **A**utomated **S**porozoite **T**racking (ToAST) that allows fully automated analysis of *Plasmodium* sporozoite movements. ToAST is based on the simple tracking of the speed and x-y position of a moving object from subsequent time frames with subsequent classification of the elementary steps of movement into 4 motility types. We developed ToAST for the purpose of tracking *Plasmodium berghei* sporozoites, which are simple crescent-shaped motile cells measuring about 12 μm in length and one μm across, and to distinguish their small set of simple movement patterns. Sporozoites are rather simple biological samples to track as they move mostly in circles. However, two other movement patterns hamper analysis if one wants to image and automatically track dozens to hundreds of actively moving (gliding) sporozoites simultaneously. Furthermore, gliding sporozoites mainly glide in an apparent counter-clockwise fashion as observed under an inverted microscope, while only a small percentage (1-5%) move in the opposite direction [26]. We were able to separate the different movement types with high reliability by simply plotting the angle between subsequent displacements over the speed of the sporozoite. Depending on image acquisition parameters (frame rate, pixel size, binning), we needed to adjust the number of frames to average over 9 time points before plotting the individual dots in a scatter plot (Fig 4B). After adjusting these parameters we achieved a high reliability in a standard sample, when 100-250 sporozoites were imaged with a 10x lens. In such an image a thresholded sporozoite consists of 30-50 \pm 15 object pixels. The accuracy of the ToAST classification is highlighted by the different outcomes between individual observers but also between different runs by a single observer, when errors in assigning patterns vary around the automatically established numbers (Fig 5 and data not shown). In order to use ToAST, the fluorescent signal should be well over the background as a low signal-to-noise ratio will cause fluctuations in coordinate detection.

4.2 Towards high throughput analysis

1
2
3
4
5
6
7
8
9
10
11
12
13
14
15
16
17
18
19
20
21
22
23
24
25
26
27
28
29
30
31
32
33
34
35
36
37
38
39
40
41
42
43
44
45
46
47
48
49
50
51
52
53
54
55
56
57
58
59
60

One of the motivations for developing ToAST was to generate a method for visual high-throughput screening to probe the effect of molecules (e.g. antibodies or chemicals) on apicomplexan parasite motility. As a proof of principle we used ToAST to reveal differences in movement patterns and speed parameters of sporozoites isolated from mosquito salivary glands at different days post infection and at different temperatures. As sporozoites show similar distribution of movement patterns and a constant gliding speed over longer times when imaged at lower temperature, we would perform larger scale analysis at 24°C rather than at 37°C. We also found that there was no detectable difference in the distribution of movement patterns between heavily infected and weakly infected salivary glands taken from mosquitoes at the same day post infection. However, differences between strongly and weakly infected mosquitoes might be revealed at different days post infection. Knowing from experience that mosquito infection underlies rather high variations we propose two sets of alternative parameters potentially leading to the same output. For mosquitoes from cages with an average infection rate for our mosquito facility we predict that it would be possible to image 40 wells of a 384 well plate each containing roughly 3,000 sporozoites for 20 seconds thus yielding information about movement parameters from around 10,000 filmed sporozoites within one hour. In order to either compensate for a bad mosquito infection rate or to simply expand the number of conditions with a given amount of parasites we suggest to alternatively use only 600 parasites per well (ca. 50 sporozoites in the field of view using a 10x objective) and film for 100 s. This procedure requires fewer mosquitoes per condition but provides a similar amount of data although image acquisition will take 5 times longer. The former procedure will likely be preferable if we want to robustly distinguish effects on different movement patterns. This could indeed be important if performing small-scale screens of compounds targeted against e.g. different myosins, which we speculate could play distinct roles in the different parasite movements or for examining different parasites.

In order to perform a full screen in a 384 well plate with 3,000 sporozoites per well and 15,000 sporozoites isolated per mosquito, 80 infected mosquitoes would have to be dissected, which an experienced technician can achieve in an hour. Note that some laboratories achieve salivary gland infection rates of up to 100,000 sporozoites per mosquito. Using a pipetting robot and an acquisition time of 20 s per movie an entire 384

1
2
3 well plate could thus be tested under ideal conditions during one working day. To achieve
4 this, sporozoites would not be added to the entire plate but in a row-by-row fashion after
5 a single row is imaged. This is based on the observation that sporozoites move reliably
6 for only about 45 min at 24°C. Movies are collected at the center of each well and stored
7 to a hard drive. A single computer (2 x 2.66 GHz Dual-Core Intel Xenon, min. 2 GB
8 RAM) would then take 6-9 hours to extract the data and another hour for visualization of
9 the complete data in Excel. Downsampling of the images during acquisition could drop
10 this time by about 4-fold, if 2x2 bins are used, which still yielded reliable results (data not
11 shown). Providing that enough insectary space and microscopy access is available, and
12 taking into account the time to rear mosquitoes, infect with *P. berghei* or *P. yoelii*, dissect
13 the salivary glands, fill the 384 well plate and evaluate the generated data, a single person
14 should be able to test up to 1000 conditions (ie. drugs) per week.

15
16
17
18
19
20
21
22
23
24
25
26
27
28
29
30
31
32
33
34
35
36
37
38
39
40
41
42
43
44
45
46
47
48
49
50
51
52
53
54
55
56
57
58
59
60
Lastly, our tracking and patterns classification tool is in principle readily adaptable to
examine other motile stages of various parasites, such as *Plasmodium* ookinetes and
Toxoplasma tachyzoites or any other cell that moves in clearly distinguishable patterns as
the tracking tool solely rests on the plotting of the displacement angle over the speed. For
the individual question or cell to be studied, however, parameters such as the number of
frames recorded per second, the pixel size and number of the chip, the number of frames
used for averaging speed or determining angular displacement have to be carefully tested
and optimized. In conclusion, we provide a procedure to probe for inhibitors of
sporozoite motility that adds a tool to those already existing for quantitative visual
screening of infected liver cells [29-31] and the classical screens focused on infected red
blood cells.

Acknowledgements

We thank Heiko Becher for advice and help on statistical analysis, Diana Scheppan for
mosquito infection, Anne Dixius, Saskia Ziegler and our undergraduate students for
manual annotation and tracking analysis and Björn Alex, Marek Cyrklaff and Sylvia
Münter for discussion and reading the manuscript. Our work is funded by grants from the
Federal German Ministry for Education and Research (BMBF – BioFuture) and the
German Research Foundation (DFG – SFB 544). Support from the Cluster of Excellence

1
2
3 CellNetworks at the University of Heidelberg and the Institute of Computational
4 Modelling at the Siberian Branch of the Russian Academy of Science is acknowledged.
5 F.F. is an affiliated member of the European Network of Excellence BioMalPar. A.S.
6 received a RISE fellowship from the German Academic Exchange Program (DAAD).
7
8
9
10
11
12
13
14
15
16
17
18
19
20
21
22
23
24
25
26
27
28
29
30
31
32
33
34
35
36
37
38
39
40
41
42
43
44
45
46
47
48
49
50
51
52
53
54
55
56
57
58
59
60

For Peer Review

Figure legends**Figure 1**

Different movement patterns of sporozoites. The right pictures represent the sum of the DIC images from the previous time points in each row. Numbers indicate time in seconds. Imaging was performed with a 63x objective, scale bar: 5 μm .

(A) Drifting. Sporozoites float passively in the medium.

(B) Attached. Sporozoites float with one end while the other end (arrow) is attached to the substrate.

(C) Waving. Sporozoites with one end attached to the substrate (arrow) while the other end is actively moving.

(D, E) Gliding. Sporozoites glide in circles either counter-clockwise (D) or clockwise (E).

Figure 2

Detection of movement patterns from low magnification movies.

(A) One half of a microscopic image of salivary gland sporozoites expressing GFP recorded with a 10x objective.

(B) Thresholded and inverted image showing signal (black) and background (white) in a 1 bit image produced from (A) using the automatic thresholder plugin (5 average deviations).

(C) Colour-coded overlay of three thresholded images recorded 4 seconds apart. Colours indicate different time points (blue 0 s, green 4 s, red 8 s). Insets highlight 3 different types of movement: attached (left), waving (right) and gliding counter-clockwise (middle).

(D) Maximum intensity projections of 20 s (white) and 100 s (red). Some sporozoites show robust gliding (right inset), while others switch between patterns over time (left inset).

(E) Sporozoites changing movement pattern over time. The percentage of sporozoites changing their pattern of movement over a 20 s period is constantly below 1%. 108 parasites were observed for 100s from one movie (1 frame per second, 10.800 data points).

Figure 3

Reliability of manual and automated tracking of sporozoite motility

(A) Speed for a single parasite tracked three times either manually or automatically. Average speeds derived from manual tracking at the parasites tip (red) or centre (black) by 3 persons and automatic tracking at the centre (green) with 3 different threshold levels: mean + $n \times$ average deviation, $n = 5, 7, 9$. Inset shows the tracked sporozoite path. Scale bar = 10 μm .

(B) Median speeds and average standard deviations of a single sporozoite tracked either at the tip manually by 3 persons once (tip, 1t 3p), by one person 3 times (tip, 3t 1p), at the centre by 3 persons once (centre, 1t 3p) or automatically with 3 different thresholds (centre, 3thr Mac).

(C,D) Sources of tracking errors by under sampling (C) and over sampling (D).

(C) Scheme representing a counter-clockwise gliding sporozoite at three time points (blue, green, red). Tracking leads to shorter distances over a given amount of time when images were taken every 9 s (yellow line, under sampling) compared to every 3 seconds (white line).

(D) A scheme illustrating one possible source of tracking error from images taken at high temporal resolution. The tip of an object (green) can be tracked either by the red or blue cross. The paths differ in distance. This distance, i.e. the potential tracking error, will increase with the number of images taken between time points (over sampling).

(E) Maximum intensity projections (100 frames at 1 Hz) of different motility patterns as imaged through a 10x objective. The upper panel shows the three simple patterns of 'attached', 'waving' and 'gliding' parasites; the lower panel displays more complex patterns consisting of linear combinations of the three simple patterns. Scale bar = 10 μm .

(F) Results of manual assignments of the movement patterns in (E). The agreement between two individuals differs between inexperienced and experienced users (inexp. and exp. u.) and between simple and complex movement patterns (simple and complex p.). Simple patterns show the strongest agreement and have a low variation between both user groups (Bright bars and data not shown). The agreement when classifying complex patterns drops for both user groups (dark and black bars) when comparing to simple

1
2
3 patterns, though experienced users perform better for all movement features (black bars).
4
5 Waving shows the lowest values and never exceeds 60% agreement between two users.
6
7 The dataset with simple (difficult) movement patterns contained 5 (7) sporozoites and
8
9 900 (1018) data points. Each track was assigned to one of the motility states by 2.6
10
11 inexperienced and 5 experienced users.
12
13
14
15
16
17
18
19
20
21
22
23
24
25
26
27
28
29
30
31
32
33
34
35
36
37
38
39
40
41
42
43
44
45
46
47
48
49
50
51
52
53
54
55
56
57
58
59
60

For Peer Review

Figure 4

Principle of automated classification of sporozoite movement patterns

(A) A scheme representing digital calculation of speed v and angle α from 3 consecutive images. Scale bar = 10 μm .

(B) Scatter plot of absolute values of the relative angle increment α plotted against speed v for sporozoites showing either attached (A, green), waving (W, red) or gliding (G, blue) pattern. Small dots display raw data points, while large dots represent averages over 9 time points. Black lines indicate the separating thresholds: attached parasites move slower than $v = 0.5 \mu\text{m/s}$ (A, vertical line); gliding sporozoites show a strong correlation of α and v and are thus separated from wavers by an intersection line through the origin ($\alpha = 0.022V$).

(C) Series of maximum intensity projections displaying a switching motility pattern of a sporozoite. The sporozoite glides in a wide counter-clockwise circle for 18 s (left panel, red arrow indicates direction of movement), waves for another 23 s (second panel) and glides clockwise describing a small circle for 22 s (third panel, green arrow indicates direction of movement). The right projection represents a coloured merge of the first three panels (red = counter-clockwise, blue = waving, green = clockwise). Numbers indicate time intervals in seconds.

(D) $v - \text{abs}(\alpha)$ scatter for the sporozoite described in (C). Subsequent data points that were averaged over 9 time points are connected according to the colour code from (C).

(E) $v - \alpha$ scatter for the sporozoite from (C) to distinguish directionally gliding. Negative values correspond to counter-clockwise (CCW), positive values to clockwise (CW) motility. Values, which were not assigned to gliding in (D) are not considered for classification, though still represented via empty circles. Arrows indicate false negative CCW gliders (red circle) and false positive wavers (filled blue circles).

(F,G) Automated image analysis and data processing pipeline.

(F) A scheme of consecutive steps with indication of the implementation level.

(G) Command windows of the thresholding and main processing plugins for ImageJ with the parameters used for tracking sporozoites at 10x magnification.

Figure 5

Reliability of ToAST versus manual classification

(A) The fit of classification of motility states for the “difficult-to-classify” parasites from Figure 3F by inexperienced and experienced users compared to the ToAST-plugin.

(B) Fit of the overall percentages of motility states for 100 parasites imaged over 100 seconds. The majority of sporozoites display a simple movement pattern. Note the automated classification varies only little when using different thresholds (average thresholds values with $n = 5, 7, 9$)

For Peer Review

Figure 6

Sporozoite movement patterns and gliding speed vary with temperature, time, origin and age of the parasites.

(A) Mosquitoes (22 days after infection) harboring GFP expressing sporozoites display weak (left) and strong (right) levels of green fluorescence. Pictures were taken with identical exposure times. Salivary gland infection of the mosquito on the left could only be detected after dissection.

(B) Quantitative analysis reveals that there is no difference in the motility pattern between parasites obtained from poorly (left inset) and highly (right inset) infected salivary glands. At this age of infection the speed of the sporozoites was not significantly different ($0.78 \mu\text{m/s} \pm 0.04 \mu\text{m/s}$ versus $0.63 \mu\text{m/s} \pm 0.1 \mu\text{m/s}$ for sporozoites from highly and poorly infected glands, respectively; $p\text{-value} = 0.11$). Insets show dissected heads with infected salivary glands still attached. Pictures were made using identical exposure times. Three highly and three poorly infected mosquitoes from the same age (22 days after infection) and cage were dissected, sporozoites were filmed and analyzed with ToAST using identical parameters. Average number of data points: 15700 for highly infected glands, 9500 for low infected, the experiments were performed in triplicates.

(C, D) Comparison of sporozoite CCW movement (C) and speed (D) at the indicated temperatures. At room temperature sporozoites describe a linear decrease in their rate of CCW movement (dropping rate: ca. 0.68 %/min). An area with parasites was filmed for 100 s at 1 Hz every 10 min for a total of 90 min.

(E) ToAST reveals differences in movement patterns according to their state of maturation. Immature sporozoites dissected from midguts show close to no effective movement (black bars). Parasites from the hemolymph show a pattern intermediate to those from midgut and salivary gland sporozoites. Error bars represent S.E.M. from three experiments.

(F) Plot of the average speeds of parasites, that were classified as either waving (light grey bars) or actively moving (black bars) in (E). Mature sporozoites (salivary glands) move and wave about 40-50% faster than those dissected from midguts and hemolymph ($p\text{-values} < 0.001$). Error bars represent S.E.M. from three experiments. The data points contributing to each average speed are plotted on the right Y-axis (grey boxes).

1
2
3 (G) Differences in movement patterns of sporozoites isolated from salivary glands at
4 different times after mosquito infection. Older sporozoites (19 days after infection, black
5 bars) show a shifted pattern with mostly counter-clockwise gliding parasites. Asterisks
6 indicate highly significant shifts in the respective pattern (p-value < 0.01). Experiments
7 were performed using parasites of the same age from three independently bred and
8 infected mosquito cages. Note the small standard deviation.
9

10
11 (H) ToAST allows rapid evaluation of the effect of cytochalasin D on sporozoite gliding.
12 All values represent the percentage of gliding parasites normalized to control parasites
13 imaged in the absence of drug. The graph shows averages of triplicates from three
14 different days using the following concentrations of cytochalasin D: 0; 0.05; 0.25; 0.75;
15 1.25 μM . The number of gliding sporozoites decreases logarithmically under the
16 influence of cytochalasin D (black trend line fits with $R^2 = 0.978$) leading to a complete
17 inhibition of movement at 1.25 μM . The graph reveals an $\text{IC}_{50} = 20 \text{ nM}$ ($\pm 10 \text{ nM}$) for
18 cytochalasin D in terms of inhibiting sporozoite gliding. Note that sporozoites gliding
19 slower than 0.5 $\mu\text{m/s}$ are not included in the analysis. 11.000 data points for every
20 condition in three independent experiments were analyzed.
21
22
23
24
25
26
27
28
29
30
31
32
33
34
35
36
37
38
39
40
41
42
43
44
45
46
47
48
49
50
51
52
53
54
55
56
57
58
59
60

5 References

- [1] Young, G. M., Badger, J. L., Miller, V. L., Motility is required to initiate host cell invasion by *Yersinia enterocolitica*. *Infect Immun* 2000, 68, 4323-4326.
- [2] Tomich, M., Herfst, C. A., Golden, J. W., Mohr, C. D., Role of flagella in host cell invasion by *Burkholderia cepacia*. *Infect Immun* 2002, 70, 1799-1806.
- [3] O'Neil, H. S., Marquis, H., *Listeria monocytogenes* flagella are used for motility, not as adhesins, to increase host cell invasion. *Infect Immun* 2006, 74, 6675-6681.
- [4] Hill, K. L., Biology and mechanism of trypanosome cell motility. *Eukaryot Cell* 2003, 2, 200-208.
- [5] Andrade, L. O., Andrews, N. W., The *Trypanosoma cruzi*-host-cell interplay: location, invasion, retention. *Nat Rev Microbiol* 2005, 3, 819-823.
- [6] Munter, S., Way, M., Frischknecht, F., Signaling during pathogen infection. *Sci STKE* 2006, re5.
- [7] Baum, J., Gilberger, T. W., Frischknecht, F., Meissner, M., Host-cell invasion by malaria parasites: insights from *Plasmodium* and *Toxoplasma*. *Trends Parasitol* 2008, 24, 557-563.
- [8] Schuler, H., Matuschewski, K., Regulation of apicomplexan microfilament dynamics by a minimal set of actin-binding proteins. *Traffic* 2006, 7, 1433-1439.
- [9] Schuler, H., Matuschewski, K., *Plasmodium* motility: actin not actin' like actin. *Trends Parasitol* 2006, 22, 146-147.
- [10] Cowman, A. F., Crabb, B. S., Invasion of red blood cells by malaria parasites. *Cell* 2006, 124, 755-766.
- [11] Vlachou, D., Schlegelmilch, T., Runn, E., Mendes, A., Kafatos, F. C., The developmental migration of *Plasmodium* in mosquitoes. *Curr Opin Genet Dev* 2006, 16, 384-391.
- [12] Matuschewski, K., Getting infectious: formation and maturation of *Plasmodium* sporozoites in the *Anopheles* vector. *Cell Microbiol* 2006, 8, 1547-1556.
- [13] Vanderberg, J. P., Frevort, U., Intravital microscopy demonstrating antibody-mediated immobilisation of *Plasmodium berghei* sporozoites injected into skin by mosquitoes. *Int J Parasitol* 2004, 34, 991-996.
- [14] Amino, R., Thiberge, S., Martin, B., Celli, S., *et al.*, Quantitative imaging of *Plasmodium* transmission from mosquito to mammal. *Nat Med* 2006, 12, 220-224.
- [15] Matsuoka, H., Yoshida, S., Hirai, M., Ishii, A., A rodent malaria, *Plasmodium berghei*, is experimentally transmitted to mice by merely probing of infective mosquito, *Anopheles stephensi*. *Parasitol Int* 2002, 51, 17-23.
- [16] Medica, D. L., Sinnis, P., Quantitative dynamics of *Plasmodium yoelii* sporozoite transmission by infected anopheline mosquitoes. *Infect Immun* 2005, 73, 4363-4369.
- [17] Yamauchi, L. M., Coppi, A., Snounou, G., Sinnis, P., *Plasmodium* sporozoites trickle out of the injection site. *Cell Microbiol* 2007, 9, 1215-1222.
- [18] Sidjanski, S., Vanderberg, J. P., Delayed migration of *Plasmodium* sporozoites from the mosquito bite site to the blood. *Am J Trop Med Hyg* 1997, 57, 426-429.
- [19] Amino, R., Franke-Fayard, B., Janse, C., Waters, A., *et al.*, Imaging Parasites in Vivo, in: Shorte, S. L., Frischknecht, F. (Eds.), *Imaging Cellular and Molecular Biological Functions (Principle and Practice)*, Springer-Verlag, Berlin 2007, pp. 345-360.
- [20] Frischknecht, F., The skin as interface in the transmission of arthropod-borne

1
2
3 pathogens. *Cell Microbiol* 2007, 9, 1630-1640.

4 [21] Frischknecht, F., Baldacci, P., Martin, B., Zimmer, C., *et al.*, Imaging movement of
5 malaria parasites during transmission by Anopheles mosquitoes. *Cell Microbiol* 2004, 6,
6 687-694.

7
8 [22] Amino, R., Menard, R., Frischknecht, F., In vivo imaging of malaria parasites--
9 recent advances and future directions. *Curr Opin Microbiol* 2005, 8, 407-414.

10 [23] Prudencio, M., Rodriguez, A., Mota, M. M., The silent path to thousands of
11 merozoites: the Plasmodium liver stage. *Nat Rev Microbiol* 2006, 4, 849-856.

12 [24] Kappe, S. H., Buscaglia, C. A., Nussenzweig, V., Plasmodium sporozoite molecular
13 cell biology. *Annu Rev Cell Dev Biol* 2004, 20, 29-59.

14 [25] Yoeli, M., Movement of the Sporozoites of Plasmodium Berghei (Vincke Et Lips,
15 1948). *Nature* 1964, 201, 1344-1345.

16 [26] Vanderberg, J. P., Studies on the motility of Plasmodium sporozoites. *J Protozool*
17 1974, 21, 527-537.

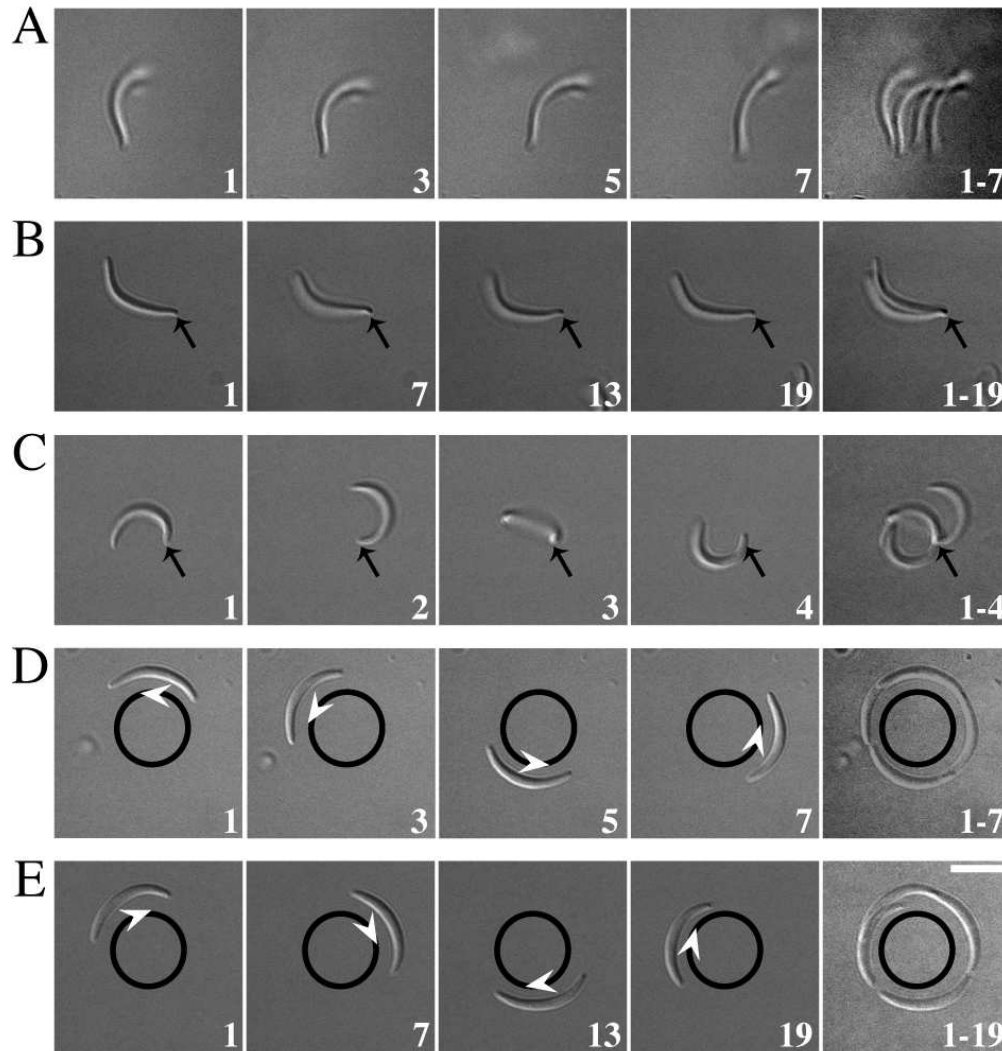
18 [27] Natarajan, R., Thathy, V., Mota, M. M., Hafalla, J. C., *et al.*, Fluorescent
19 Plasmodium berghei sporozoites and pre-erythrocytic stages: a new tool to study
20 mosquito and mammalian host interactions with malaria parasites. *Cell Microbiol* 2001,
21 3, 371-379.

22 [28] Russell, D. G., Sinden, R. E., The role of the cytoskeleton in the motility of
23 coccidian sporozoites. *J Cell Sci* 1981, 50, 345-359.

24 [29] Prudencio, M., Rodrigues, C. D., Hannus, M., Martin, C., *et al.*, Kinome-wide RNAi
25 screen implicates at least 5 host hepatocyte kinases in Plasmodium sporozoite infection.
26 *PLoS Pathog* 2008, 4, e1000201.

27 [30] Cunha-Rodrigues, M., Prudencio, M., Mota, M. M., Haas, W., Antimalarial drugs -
28 host targets (re)visited. *Biotechnol J* 2006, 1, 321-332.

29 [31] Gego, A., Silvie, O., Franetich, J. F., Farhati, K., *et al.*, New approach for high-
30 throughput screening of drug activity on Plasmodium liver stages. *Antimicrob Agents*
31 *Chemother* 2006, 50, 1586-1589.
32
33
34
35
36
37
38
39
40
41
42
43
44
45
46
47
48
49
50
51
52
53
54
55
56
57
58
59
60



Different movement patterns of sporozoites.

The right pictures represent the sum of the DIC images from the previous time points in each row. Numbers indicate time in seconds. Imaging was performed with a 63x objective, scale bar: 5 μm .

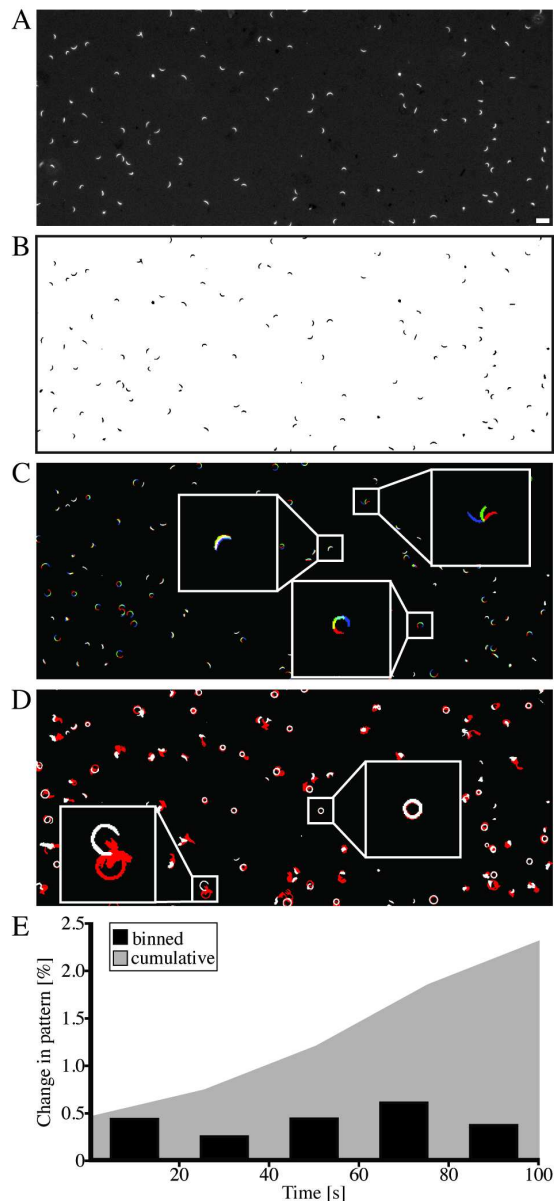
(A) Drifting. Sporozoites float passively in the medium.

(B) Attached. Sporozoites float with one end while the other end (arrow) is attached to the substrate.

(C) Waving. Sporozoites with one end attached to the substrate (arrow) while the other end is actively moving.

(D, E) Gliding. Sporozoites glide in circles either counter-clockwise (D) or clockwise (E).

79x84mm (300 x 300 DPI)



Detection of movement patterns from low magnification movies.

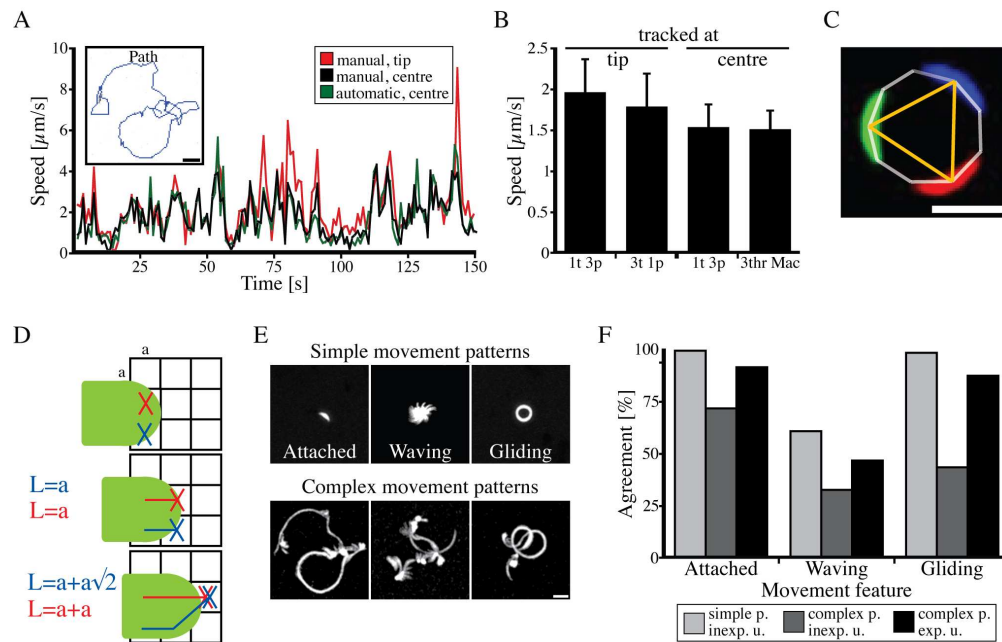
- (A) One half of a microscopic image of salivary gland sporozoites expressing GFP recorded with a 10x objective.
- (B) Thresholded and inverted image showing signal (black) and background (white) in a 1 bit image produced from (A) using the automatic thresholder plugin (5 average deviations).
- (C) Colour-coded overlay of three thresholded images recorded 4 seconds apart. Colours indicate different time points (blue 0 s, green 4 s, red 8 s). Insets highlight 3 different types of movement: attached (left), waving (right) and gliding counter-clockwise (middle).
- (D) Maximum intensity projections of 20 s (white) and 100 s (red). Some sporozoites show robust gliding (right inset), while others switch between patterns over time (left inset).
- (E) Sporozoites changing movement pattern over time. The percentage of sporozoites changing their pattern of movement over a 20 s period is constantly below 1%. 108 parasites were observed

for 100s from one movie (1 frame per second, 10.800 data points).

79x176mm (300 x 300 DPI)

For Peer Review

1
2
3
4
5
6
7
8
9
10
11
12
13
14
15
16
17
18
19
20
21
22
23
24
25
26
27
28
29
30
31
32
33
34
35
36
37
38
39
40
41
42
43
44
45
46
47
48
49
50
51
52
53
54
55
56
57
58
59
60



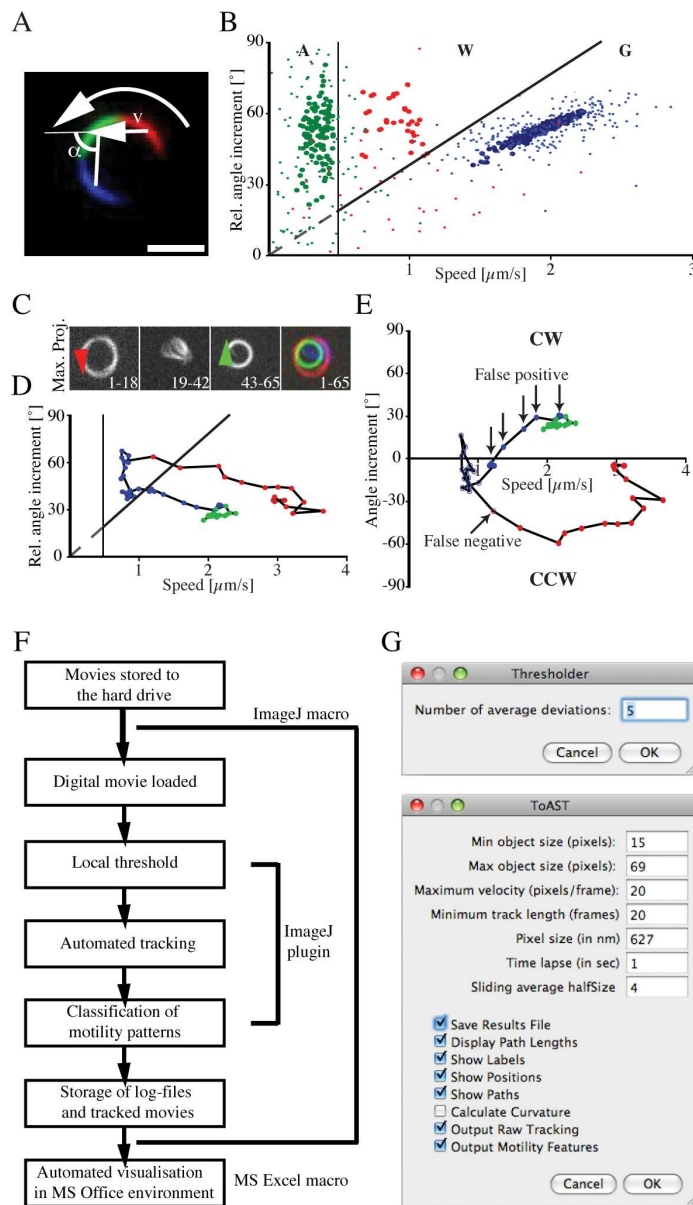
Reliability of manual and automated tracking of sporozoite motility

- (A) Speed for a single parasite tracked three times either manually or automatically. Average speeds derived from manual tracking at the parasites tip (red) or centre (black) by 3 persons and automatic tracking at the centre (green) with 3 different threshold levels: mean + $n \times$ average deviation, $n = 5, 7, 9$. Inset shows the tracked sporozoite path. Scale bar = $10 \mu\text{m}$.
- (B) Median speeds and average standard deviations of a single sporozoite tracked either at the tip manually by 3 persons once (tip, 1t 3p), by one person 3 times (tip, 3t 1p), at the centre by 3 persons once (centre, 1t 3p) or automatically with 3 different thresholds (centre, 3thr Mac).
- (C,D) Sources of tracking errors by under sampling (C) and over sampling (D).
- (C) Scheme representing a counter-clockwise gliding sporozoite at three time points (blue, green, red). Tracking leads to shorter distances over a given amount of time when images were taken every 9 s (yellow line, under sampling) compared to every 3 seconds (white line).
- (D) A scheme illustrating one possible source of tracking error from images taken at high temporal resolution. The tip of an object (green) can be tracked either by the red or blue cross. The paths differ in distance. This distance, i.e. the potential tracking error, will increase with the number of images taken between time points (over sampling).
- (E) Maximum intensity projections (100 frames at 1 Hz) of different motility patterns as imaged through a 10x objective. The upper panel shows the three simple patterns of 'attached', 'waving' and 'gliding' parasites; the lower panel displays more complex patterns consisting of linear combinations of the three simple patterns. Scale bar = $10 \mu\text{m}$.
- (F) Results of manual assignments of the movement patterns in (E). The agreement between two individuals differs between inexperienced and experienced users (inexp. and exp. u.) and between simple and complex movement patterns (simple and complex p.). Simple patterns show the strongest agreement and have a low variation between both user groups (Bright bars and data not shown). The agreement when classifying complex patterns drops for both user groups (dark and black bars) when comparing to simple patterns, though experienced users perform better for all movement features (black bars). Waving shows the lowest values and never exceeds 60% agreement between two users. The dataset with simple (difficult) movement patterns contained 5 (7) sporozoites and 900 (1018) data points. Each track was assigned to one of the motility states by 2.6 inexperienced and 5 experienced users.

171x109mm (300 x 300 DPI)

1
2
3
4
5
6
7
8
9
10
11
12
13
14
15
16
17
18
19
20
21
22
23
24
25
26
27
28
29
30
31
32
33
34
35
36
37
38
39
40
41
42
43
44
45
46
47
48
49
50
51
52
53
54
55
56
57
58
59
60

For Peer Review



Principle of automated classification of sporozoite movement patterns

(A) A scheme representing digital calculation of speed v and angle α from 3 consecutive images. Scale bar = 10 μm .

(B) Scatter plot of absolute values of the relative angle increment α plotted against speed v for sporozoites showing either attached (A, green), waving (W, red) or gliding (G, blue) pattern. Small dots display raw data points, while large dots represent averages over 9 time points. Black lines indicate the separating thresholds: attached parasites move slower than $v = 0.5 \mu\text{m/s}$ (A, vertical line); gliding sporozoites show a strong correlation of α and v and are thus separated from wavers by an intersection line through the origin ($\alpha = 0.022V$).

(C) Series of maximum intensity projections displaying a switching motility pattern of a sporozoite. The sporozoite glides in a wide counter-clockwise circle for 18 s (left panel, red arrow indicates direction of movement), waves for another 23 s (second panel) and glides clockwise describing a

1
2
3 small circle for 22 s (third panel, green arrow indicates direction of movement). The right projection
4 represents a coloured merge of the first three panels (red = counter-clockwise, blue = waving,
5 green = clockwise). Numbers indicate time intervals in seconds.

6 (D) $v - \text{abs}(a)$ scatter for the sporozoite described in (C). Subsequent data points that were
7 averaged over 9 time points are connected according to the colour code from (C).

8 (E) $v - a$ scatter for the sporozoite from (C) to distinguish directionally gliding. Negative values
9 correspond to counter-clockwise (CCW), positive values to clockwise (CW) motility. Values, which
10 were not assigned to gliding in (D) are not considered for classification, though still represented via
11 empty circles. Arrows indicate false negative CCW gliders (red circle) and false positive wavers
12 (filled blue circles).

13 (F,G) Automated image analysis and data processing pipeline.

14 (F) A scheme of consecutive steps with indication of the implementation level.

15 (G) Command windows of the thresholding and main processing plugins for ImageJ with the
16 parameters used for tracking sporozoites at 10x magnification.

17 99x173mm (300 x 300 DPI)

18
19
20
21
22
23
24
25
26
27
28
29
30
31
32
33
34
35
36
37
38
39
40
41
42
43
44
45
46
47
48
49
50
51
52
53
54
55
56
57
58
59
60

For Peer Review

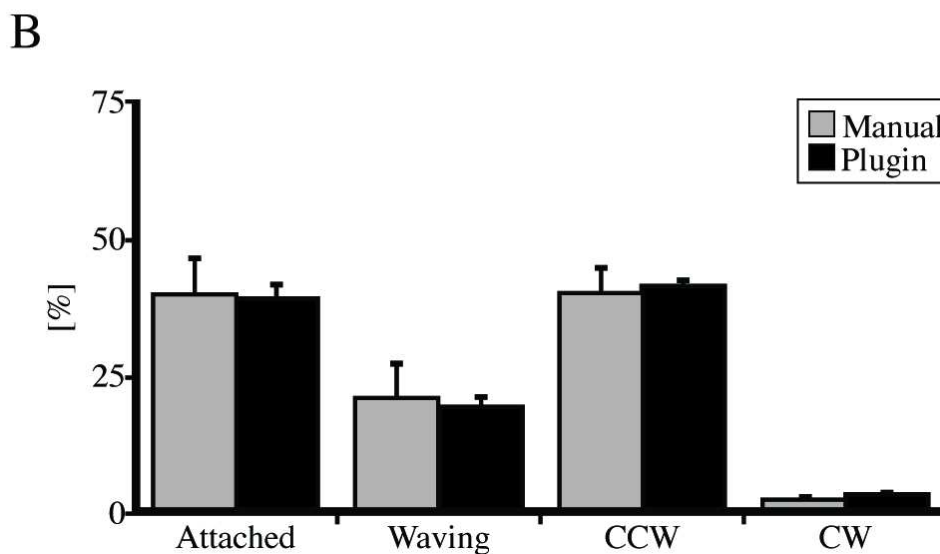
A

Inexperienced users

		%	Attached	Waving	Gliding
Plugin	Attached		72	12	17
	Waving		59	32	8
	Gliding		49	8	43

Experienced users

		%	Attached	Waving	Gliding
Plugin	Attached		90	8	2
	Waving		56	29	15
	Gliding		37	6	58



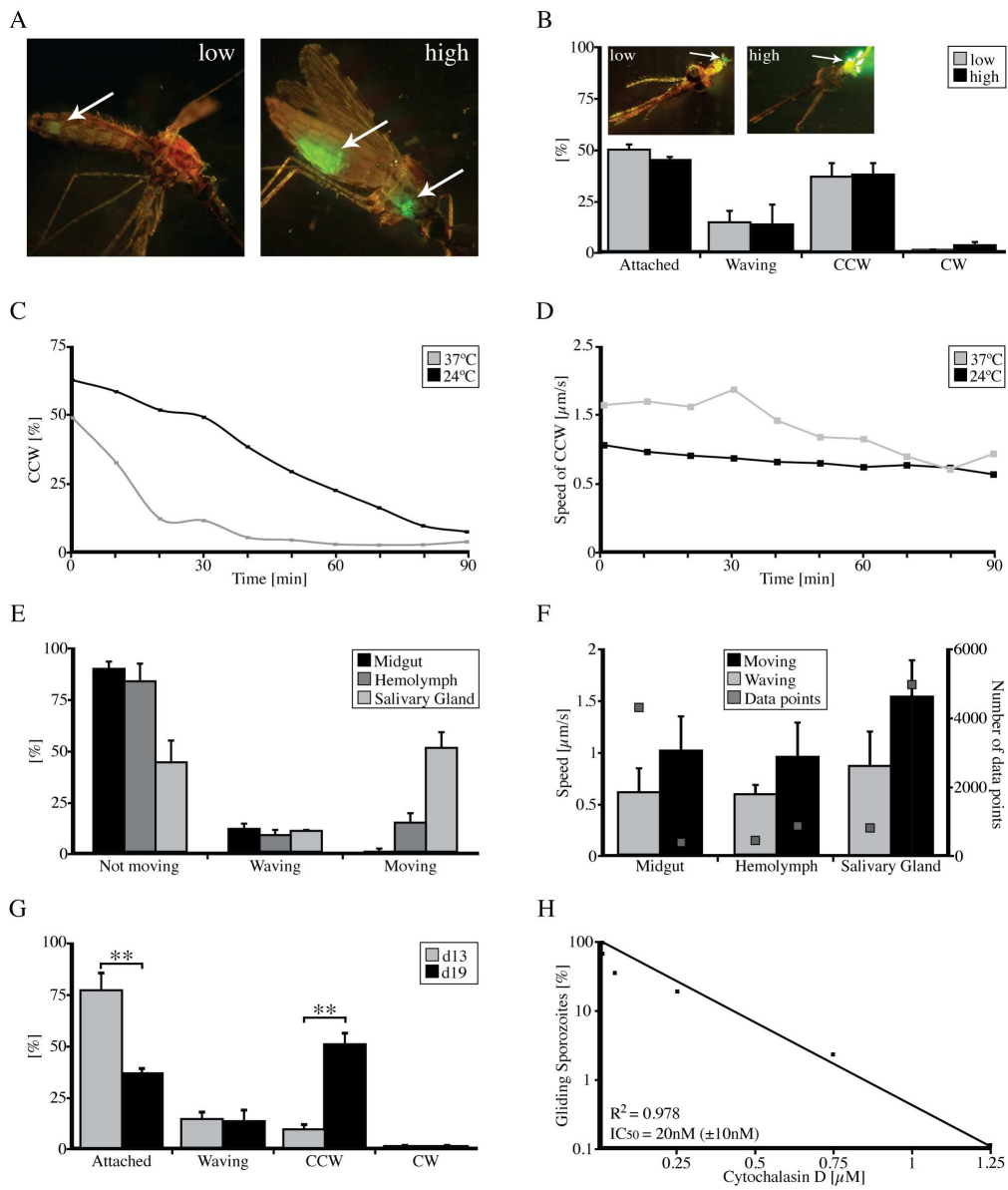
Reliability of ToAST versus manual classification

(A) The fit of classification of motility states for the "difficult-to-classify" parasites from Figure 3F by inexperienced and experienced users compared to the ToAST-plugin.

(B) Fit of the overall percentages of motility states for 100 parasites imaged over 100 seconds. The majority of sporozoites display a simple movement pattern. Note the automated classification varies only little when using different thresholds (average threshold values with $n = 5, 7, 9$)

80x101mm (300 x 300 DPI)

1
2
3
4
5
6
7
8
9
10
11
12
13
14
15
16
17
18
19
20
21
22
23
24
25
26
27
28
29
30
31
32
33
34
35
36
37
38
39
40
41
42
43
44
45
46
47
48
49
50
51
52
53
54
55
56
57
58
59
60



169x200mm (300 x 300 DPI)